APC16 is a conserved subunit of the anaphase-promoting complex/cyclosome

Geert J. P. L. Kops[1],*,‡, Monique van der Voet[2],§, Michael S. Manak[3,4],§, Maria H. J. van Osch[1], Said M. Naini[4], Andrea Brear[3,4], Ian X. McLeod[5], Dirk M. Hentschel[4], John R. Yates, III[5], Sander van den Heuvel[2] and Jagesh V. Shah[3,4],*,‡

[1]Department of Physiological Chemistry and Cancer Genomics Centre, UMC Utrecht, Utrecht, The Netherlands
[2]Developmental Biology, Utrecht University, The Netherlands
[3]Department of Systems Biology, Harvard Medical School, Boston, MA 02115, USA
[4]Renal Division, Brigham and Women's Hospital, Harvard Medical School, Boston MA 02115, USA
[5]Department of Cell Biology, The Scripps Research Institute, La Jolla, CA 92037, USA
*These authors contributed equally to this work
‡Authors for correspondence (g.j.p.l.kops@umcutrecht.nl; jagesh@hms.harvard.edu)
§These authors contributed equally to this work

Summary

Error-free chromosome segregation depends on timely activation of the multi-subunit E3 ubiquitin ligase APC/C. Activation of the APC/C initiates chromosome segregation and mitotic exit by targeting critical cell-cycle regulators for destruction. The APC/C is the principle target of the mitotic checkpoint, which prevents segregation while chromosomes are unattached to spindle microtubules. We now report the identification and characterization of APC16, a conserved subunit of the APC/C. APC16 was found in association with tandem-affinity-purified mitotic checkpoint complex protein complexes. APC16 is a bona fide subunit of human APC/C: it is present in APC/C complexes throughout the cell cycle, the phenotype of APC16-depleted cells copies depletion of other APC/C subunits, and APC16 is important for APC/C activity towards mitotic substrates. APC16 sequence homologues can be identified in metazoans, but not fungi, by four conserved primary sequence stretches. We provide evidence that the *C. elegans* gene K10D2.4 and the *D. rerio* gene zgc:110659 are functional equivalents of human APC16. Our findings show that APC/C is composed of previously undescribed subunits, and raise the question of why metazoan APC/C is molecularly different from unicellular APC/C.

Key words: Anaphase-promoting complex, Spindle-assembly checkpoint, E3 ubiquitin ligase, Metaphase-to-anaphase transition, Tandem-affinity purification

Introduction

Timely destruction of cell cycle regulators by the proteasome is integral to successful cell division in all eukaryotes. One of the machineries that promotes protein destruction is the E3 ubiquitin ligase anaphase-promoting complex/cyclosome or APC/C (Peters, 2006). The APC/C poly-ubiquitylates protein substrates that are recognized by its coactivator proteins Cdc20 and Cdh1 (Fang et al., 1998b; Kramer et al., 1998; Visintin et al., 1997). Originally identified by its ability to ubiquitylate cyclin B and thus promote chromosome segregation in mitosis (Irniger et al., 1995; King et al., 1995; Sudakin et al., 1995), the APC/C has since been shown to have many additional targets in mitosis as well as in interphase. Targets of APC/C^{Cdc20} include cyclin A, HOXC10 and Nek2A in the early stages of mitosis (den Elzen and Pines, 2001; Gabellini et al., 2003; Geley et al., 2001; Hames et al., 2001) and cyclin B, securin and Kid during metaphase (Clute and Pines, 1999; Cohen-Fix et al., 1996; Funabiki and Murray, 2000; Funabiki et al., 1996; Hagting et al., 2002; Yamamoto et al., 1996; Zou et al., 1999; Zur and Brandeis, 2001). Shortly thereafter, in early anaphase, Cdh1 takes over from Cdc20 (Hagting et al., 2002) and aides the APC/C in ubiquitylating a variety of substrates in late mitosis or interphase that include aurora B, Plk1, Cdc20, Mps1 and geminin (Lindon and Pines, 2004; McGarry and Kirschner, 1998; Palframan et al., 2006; Pfleger and Kirschner, 2000; Prinz et al., 1998; Stewart and Fang, 2005; Zielke et al., 2008) [a list of additional APC/C^{Cdh1}

substrates is provided by Li and Zhang (Li and Zhang, 2009)]. By ensuring destruction of these proteins, the APC/C is responsible for timely chromosome disjunction and mitotic exit (e.g. cyclins and securin), as well as for coordination of events that initiate a single round of DNA replication (e.g. cyclin A and geminin). Although recently challenged (Walker et al., 2008), the APC/C is proposed to auto-inhibit by targeting its associated E2 ubiquitin conjugating enzyme UbcH10 for destruction in late G1, allowing essential cell cycle regulators such as cyclin A to accumulate during S phase (Rape and Kirschner, 2004).

The APC/C^{Cdc20} is the principal target of the mitotic (or spindle assembly) checkpoint, a surveillance mechanism that ensures that cells cannot initiate chromosome segregation until all chromosomes are stably attached to spindle microtubules (Musacchio and Salmon, 2007). Unattached chromosomes catalyse production of an APC/C inhibitor termed mitotic checkpoint complex (MCC), thus preventing premature chromosome segregation and mitotic exit (Hardwick et al., 2000; Kulukian et al., 2009; Sudakin et al., 2001). The mitotic checkpoint protein BubR1 (also known as BUB1β; in complex with Bub3) is an essential component of the MCC as it directly binds Cdc20 and inhibits APC/C activity in vitro (Fang, 2002; Kulukian et al., 2009; Tang et al., 2001a). In cells, the inhibitory activity of BubR1 requires Mad2 to visit unattached kinetochores, and in vitro Mad2 strongly stimulates the ability of BubR1 to

inhibit the APC/C (De Antoni et al., 2005; Fang, 2002; Kulukian et al., 2009). Although evidence to the contrary exists (Nilsson et al., 2008), Mad2 might in addition be part of the MCC, as it has been found in APC/C complexes (Herzog et al., 2009) and can inhibit APC/C activity in vitro (Fang et al., 1998a; Herzog et al., 2009). In addition to its composition, the mode of inhibition of APC/C by the MCC is not fully understood. It is mediated by Cdc20 interactions (Kulukian et al., 2009) and requires recognition of the KEN box motifs of BubR1 that in other proteins can function as a destruction signal for APC/C substrates (Burton and Solomon, 2007; King et al., 2007; Malureanu et al., 2009). The MCC partly replaces Cdc20 from its normal binding site on the APC/C complex, diminishes UbcH10 binding and substrate binding, and imposes a structural rearrangement that puts APC/C in a closed conformational state (Herzog et al., 2009). Whether these structural changes are sufficient to explain the potent inhibition of APC/C activity by the MCC remains to be investigated.

The APC/C is a complex 20S multisubunit assembly (Peters, 2006). The APC/C is composed of at least 11 subunits, which are conserved between yeast and vertebrates: APC1-6, APC8, APC10, APC11, APC13 and Cdc26. Four of these (APC3/Cdc27, APC6/Cdc16, APC8/Cdc23 and Cdc26) in addition to the coactivator protein Cdc20 had previously been identified as *CDC* mutants that caused G2-M delays in the genetic screens by Hartwell and colleagues (Hartwell et al., 1974; Irniger et al., 1995; King et al., 1995; Lamb et al., 1994; Sudakin et al., 1995; Tugendreich et al., 1995; Zachariae et al., 1998; Zachariae et al., 1996). Three of the four 'CDC' subunits of the APC/C have tetratricopeptide (TPR) repeats (Lamb et al., 1994) and are involved in coactivator binding (Thornton et al., 2006; Vodermaier et al., 2003). E3 ligase activity can be reconstituted in vitro by a two-subunit complex composed of the scaffold APC2 and APC11 that have cullin homology and ring-finger motifs, respectively (Gmachl et al., 2000; Leverson et al., 2000; Tang et al., 2001b; Yu et al., 1998). This catalytic module functions in concert with three E2 ubiquitin conjugating enzymes to poly-ubiquitylate substrates. Ubiquitylation is initiated by the E2 enzymes UBE2C/UbcH10 and UBE2D1/UbcH5, while ubiquitin chains are further elongated by Ube2S (Aristarkhov et al., 1996; Garnett et al., 2009; Irniger et al., 1995; King et al., 1995; Osaka et al., 1997; Townsley et al., 1997; Williamson et al., 2009; Wu et al., 2010; Yu et al., 1996). Finally, the small subunit APC10 may be involved in APC/C processivity and/or substrate recognition (Carroll and Morgan, 2002; Matyskiela and Morgan, 2009; Passmore et al., 2003). It is unclear what role the other subunits fulfill in APC/C functionality, but most are essential for budding yeast viability [see Thornton and Toczyski (Thornton and Toczyski, 2003) and references therein].

In addition to the 11 'core' subunits that are found in APC/C complexes in metazoans, plants and fungi (reviewed by Capron et al., 2003; Peters, 2006), additional species-specific subunits have been identified. APC9 associates with the APC/C in several fungi including budding yeast and promotes efficient ubiquitylation of some but not all mitotic budding yeast APC/C substrates (Page et al., 2005). Likewise, APC14 is a bona fide APC/C component in fission yeast only (Yoon et al., 2002), and both yeast model organisms, but not metazoans, have an additional, related APC/C subunit, termed Mnd2 in budding yeast or APC15 in fission yeast (Page et al., 2005; Yoon et al., 2002). Mnd2 is required for APC/C function in meiosis (Yoon et al., 2002). Finally, APC/C complexes

in Metazoa and plants but not fungi contain APC7, a fourth TPR-domain containing protein that, like the other TPR subunits, participates in coactivator binding in human cells (Vodermaier et al., 2003; Yoon et al., 2002; Yu et al., 1998).

We set out to identify the minimal MCC-APC/C complex in humans by comparing tandem-affinity purifications of Mad2- and BubR1-containing complexes from mitotic human cells. This revealed the presence of C10orf104, recently identified as MSAG (metabolic syndrome associated gene) by differential cDNA expression screening of liver genes that respond to high glucose (Cui et al., 2009). Here we show that C10orf104 (MSAG) is a bona fide APC/C subunit in human cells and as such we have renamed it APC16. APC16 is conserved in metazoans and possibly plants but no apparent homologue has been found in fungi, and we show functional conservation of APC16 in *Caenorhabditis elegans* and *Danio rerio*.
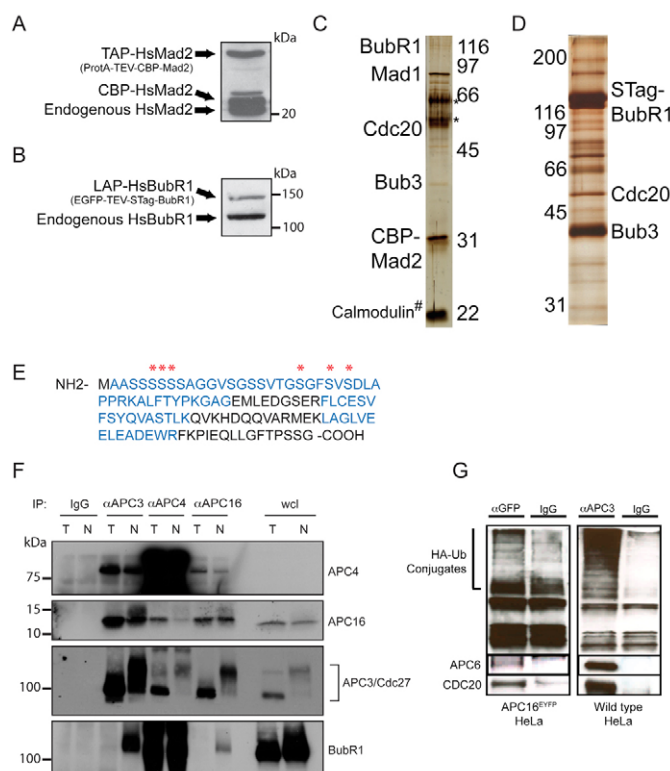

Fig. 1. Tandem-affinity purifications of MCC-APC/C identifies the APC/C interactor C10orf104 (APC16). (A,B) Expression levels of TAP-tagged Mad2 (A) and LAP-tagged BubR1 (B) relative to the endogenous proteins. (C,D) SDS-PAGE silver staining of tandem-affinity purifications of Mad2 (C) and BubR1 (D) from mitotic HeLa cells. Molecular mass markers as well as some of the interactors are indicated. (E) Primary amino acid sequence of APC16. Blue indicates sequences covered in the various mass spectrometry analyses. Red asterisks indicates phosphorylated residues. (F) Immunoblots (APC4, APC16, BubR1 or APC3/Cdc27) of the various immunoprecipitates (IP) and of whole-cell lysates (wcl) from mitotic (nocodazole, N) or interphase (thymidine, T) HeLa cells. (G) Anti-GFP immunoprecipitates from APC16^EYFP-expressing HeLa cells incubated with a recombinant securin substrate resulted in a HA-ubiquitin banding pattern consistent with ubiquitylation. Anti-APC3 immunoprecipitates also contained ubiquitylation activity whereas control IgG precipitates did not. The immunoprecipitates with ubiquitylation activity also contained Cdc20 and APC6/Cdc16.

Results

Tandem-affinity purification of MCC complexes identifies C10orf104

To examine the protein composition of MCC-containing complexes, the MCC was tandem-affinity purified from mitotic HeLa cell lines that stably expressed Mad2 or BubR1 fused to the tandem-affinity purification tag TAP or LAP, respectively (Fig. 1A-D; supplementary material Fig. S1). Proteolytic digestions of urea eluates were then processed for peptide identification by mass spectrometry. Present in the TAP-Mad2 purifications were the direct Mad2 interactors Mad1 and p31comet (Chen et al., 1998; Habu et al., 2002) as well as TPR (Lee et al., 2008), PRP4 (Montembault et al., 2007) and ZW10, KNL1 (blinkin) and Rae1 (Table 1). BubR1 interactors included the direct interactor KNL1 (Kiyomitsu et al., 2007) and Bub1 (Taylor et al., 2001). Although some of the proteins found in the TAP-Mad2 purifications are predicted to be specific for Mad2 association, because fewer cells were used for the BubR1 pull-downs (supplementary material Fig. S1) it cannot be excluded that some proteins detected solely in the TAP-Mad2 purifications also associated with BubR1-containing complexes, yet failed to be sufficiently covered. Overlay of all identified proteins from the separate purifications pinpointed a number of proteins that were present in both samples at high coverage and that thus probably constituted the MCC-associated protein complexes. As expected (Herzog et al., 2009), all MCC components including Bub3 and Cdc20, as well as the majority of APC/C subunits were present. Notable exceptions were APC11 and APC13, perhaps because of difficulty in detection owing to a

combination of their small size (9.8 and 8.5 kDa, respectively) and amino acid composition, as previously noted (Kraft et al., 2003). Consistently present in all purifications was the previously uncharacterized 11.7 kDa protein C10orf104, which we have renamed APC16 (see functional characterizations below; Table 1). In all purifications combined, we identified four peptides that together covered 61.4% of the primary APC16 sequence and contained six putative phosphorylated residues (Fig. 1E).

APC16 is a constitutive subunit of the APC/C holocomplex

To address whether APC16 behaved as a component of the MCC, the APC/C, or neither, we examined association of APC16 with APC/C complexes in mitosis and interphase. An antibody raised to APC16 recognized a ~12 kDa band that was enriched in immunoprecipitations and that was reduced in intensity upon APC16 RNAi (see below). We therefore conclude that the antibody recognizes endogenous APC16 protein. Immunoprecipitations of the APC/C using APC3/Cdc27 or APC4 antibodies coprecipitated APC16 and, vice versa, APC16 precipitations contained the APC3/Cdc27 and APC4 subunits (Fig. 1F). Since APC3/Cdc27 is part of the 'head' domain of the APC/C whereas APC4 is part of the 'platform' domain (Herzog et al., 2009), the fact that both APC3/Cdc27 and APC4 coprecipitated with APC16 indicated that the entire APC/C assembly was co-purified with APC16. In agreement with this, gelfiltration experiments showed that APC16 co-migrated with the APC/C holocomplex at around 1.5 MDa (Fig. 4B). As an alternative strategy for monitoring APC16, we generated a HeLa-derived cell line stably expressing APC16^{EYFP}. Precipitation of APC16^{EYFP} using anti-GFP antibodies and gelfiltration experiments verified its association with APC/C complexes in mitotic cells (supplementary material Fig. S2A-C) Importantly, APC16^{EYFP} precipitations from these cells co-purified E3 ubiquitin ligase activity (Fig. 1G). To our knowledge, this is only the second report of incorporation of a tagged subunit into the APC/C in human cells, the first being APC8 (Poser et al., 2008). Endogenous APC16 was found associated with APC3/Cdc27 and APC4 in interphase, thymidine-blocked cells, as well as in mitotic, nocodazole-blocked cells, whereas BubR1 was found associated to APC/C complexes only in mitotic cells (Fig. 1F). Similarly, APC16 immunoprecipitates from interphase as well as mitotic cells contained APC3/Cdc27 and APC4, whereas BubR1 associated with APC16-containing complexes only in mitosis (Fig. 1F). Similar results were obtained with precipitations from the APC16^{EYFP} HeLa cells (supplementary material Fig. S2). Thus, APC16 is a constitutive interactor of the APC/C in human cells.

Prolonged metaphase delays in cells depleted of APC16

Genetic inactivation of APC/C components in yeast, worms, flies and mice, and injection of anti-APC/C antibodies in mammalian cells have been reported to result in arrest at metaphase (Furuta et al., 2000; Golden et al., 2000; Irniger et al., 1995; Sigrist and Lehner, 1997; Tugendreich et al., 1995; Wirth et al., 2004). To examine whether the constitutive association of APC16 with the APC/C reflected a functional role for APC16 in APC/C activity, mitotic progression was analyzed by time-lapse microscopy of HeLa cells expressing H2B^{EYFP} upon RNAi-mediated knockdown of APC16, and compared with knockdown of established APC/C subunits. Depletion of APC16 with double-stranded siRNA oligonucleotides directed against the ORF or the 3′ or 5′ UTRs (Fig. 2A) caused strong mitotic delays in the vast majority of cells (Fig. 2B-E). The average time spent in mitosis was 45 minutes for

Table 1. Mass spectroscopic analysis of TAP-Mad2 and LAP-BubR1 purifications

Name	Molecular mass (kDa)	TAP-Mad2 coverage (%)	LAP-BubR1 coverage (%)
TAP bait			
Mad2	23.5	86.80	22.40
BubR1	119.5	38.10	57.20
MCC			
Bub3	37.2	46.00	55.80
Cdc20	54.7	45.70	22.40
APC/C			
APC1	216.5	37.20	7.50
APC2	93.8	21.50	4.10
APC3/Cdc27	91.8	34.20	7.40
APC4	92.1	55.70	5.40
APC5	85.1	49.90	5.60
APC6/Cdc16	71.5	48.10	7.40
APC7	63.2	58.80	11.70
APC8/Cdc23	68.3	53.10	11.20
APC10	21.2	30.80	ND
Cdc26	9.8	54.10	ND
Other – kinetochore			
Bub1	122.3	ND	15.90
KNL1/blinkin	265	7.70	6.20
Mad1	91.7	56.50	ND
Zwint-1	31.3	34.70	ND
Rae1	41	31.50	ND
p31comet	31.1	65.30	ND
PRP4	58.4	46.90	ND
TPR	265.6	12.30	ND
Other – uncharacterized			
c10orf104	11.7	51.80	63.70

Significant proteins were chosen based on criteria outlined in Materials and Methods except APC2, APC10 and Cdc26, which were chosen based on their association with the mitotic APC/C.
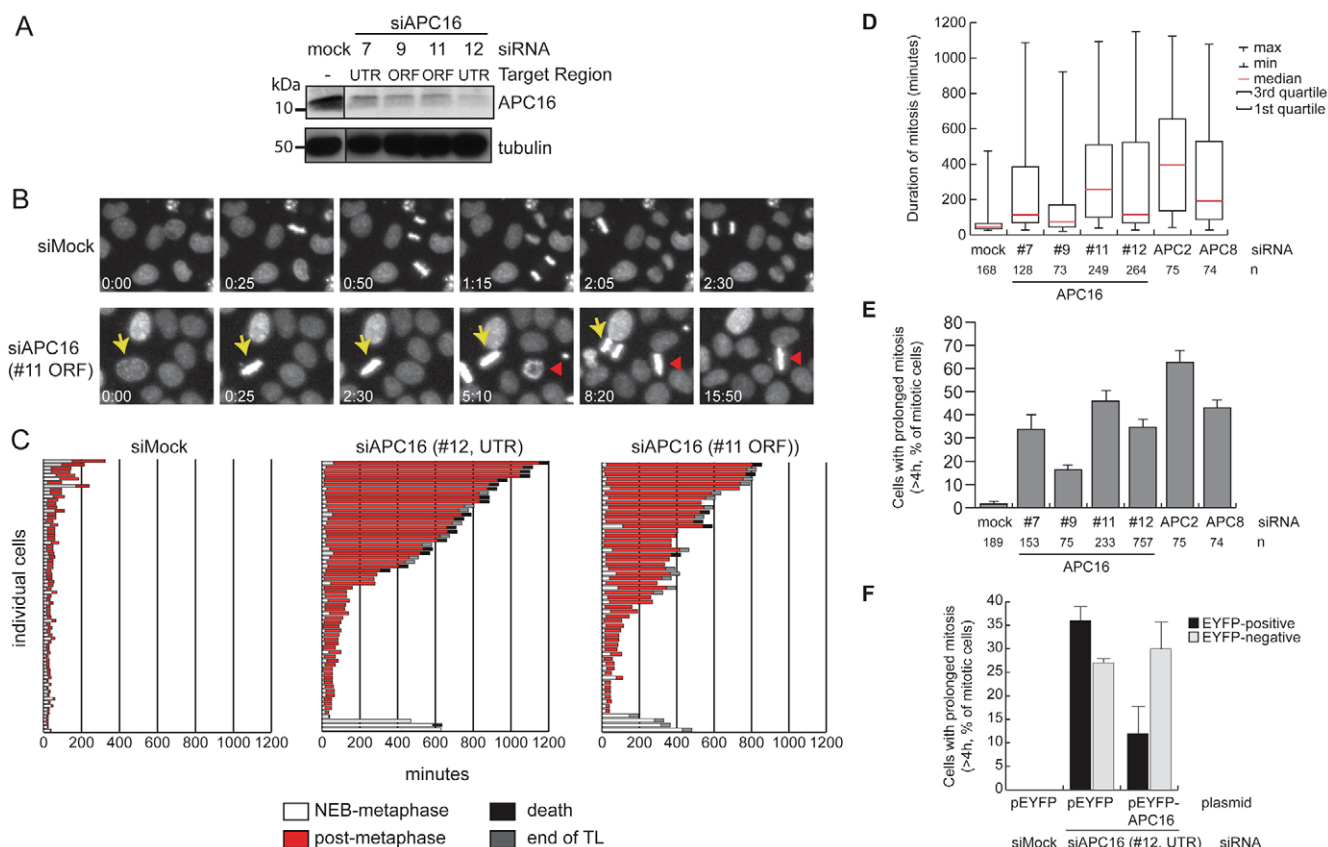
ND, not determined.

Fig. 2. APC16 depletion prevents exit from mitosis. (**A**) Immunoblots of cells transfected with the indicated siRNA oligonucleotides. UTR (untranslated region) and ORF (open reading frame) refer to location of the siRNA targeting sequence within endogenous APC16 mRNA. (**B**) Selected frames of a live cell imaging series of HeLa-H2B^{EYFP} cells either mock transfected or transfected with APC16 siRNA (#11, ORF). The arrows and arrowheads each point to a cell with a metaphases of ~8 hours (arrow) and at least 10 hours (arrowhead). (**C**) Graph of the cumulative duration of mitotic phases in cells transfected and analyzed as in B. Each bar represent one cell. Bars indicate time from nuclear envelope breakdown (NEB) to metaphase (white), from the first frame of metaphase to either anaphase, death (black, usually preceded by loss of chromosome alignment for 1-2 hours), or the end of the time-lapse (TL) experiment (gray). Red indicates post-metaphase stages. (**D**) Whisker diagram of the duration of mitosis (NEB to anaphase) in HeLa cells transfected with the indicated siRNA oligonucleotides and imaged with DIC microscopy. Cells never entering anaphase were included provided they had entered mitosis at least 6 hours before the experiment was terminated. The number of cell analyses (*n*) is indicated. Data are of at least three independent experiments. (**E**) The percentage of cells (transfected and imaged as in D) in which mitosis took longer than 4 hours. Values are means ± s.d. from at least three independent experiments. (**F**) The percentage of HeLa cells, transfected with plasmids and siRNA oligonucleotides as indicated, in which mitosis took longer than 4 hours. Values are means ± s.d. of transfected (EYFP-positive) and untransfected (EYFP-negative) cells in the same well; data are from two independent experiments.

control cells and 75, 112, 115 or 258 minutes for cells depleted of APC16 with each of the four siRNAs, respectively (Fig. 2D). Analysis of the individual stages of mitosis indicated that the delay was due to a strong increase in the time spent in metaphase, whereas the duration of prometaphase was mostly unaltered compared with cells transfected with mock siRNAs (Fig. 2B,C). The length of metaphase varied between cells, but could be as long as 18 hours (Fig. 2C,D). Long metaphase delays were often followed by loss of chromosome alignment prior to cell death (not shown). Depending on the siRNA used, 16-45% of cells with reduced APC16 delayed metaphase for more than 4 hours, compared with 1% in control cells (Fig. 2E). Importantly, in all analyses, depletion of APC8 or APC2 delayed mitosis to similar extents as APC16 depletion (Fig. 2D,E).

All four siRNA oligonucleotides to APC16 caused comparable mitotic phenotypes in cells, albeit to different extents (Fig. 2E). To further verify specificity of APC16 knockdown, the effects of an oligonucleotide targeting the 5′ UTR of APC16 (APC16si#12)

were examined in cells transiently expressing epitope-tagged APC16 lacking UTRs in the sequence. Whereas 36% of cells transfected with control plasmids were in mitosis for more than 4 hours upon APC16 depletion, only 12% of cells expressing APC16^{EYFP} were (Fig. 2F). Importantly, this threefold reduction in the fraction of cells with prolonged mitosis did not reflect sample-to-sample variation, as the untransfected cells in both preparations behaved similarly (mitosis lasted >4 hours in 27% versus 30% of cells, respectively; Fig. 2F). To our knowledge, this is the first report of a (partial) functional rescue of an APC/C-depletion phenotype in human cells. Taken together, these data support the hypothesis that APC16 is required for the metaphase-to-anaphase transition.

APC16 depletion stabilizes mitotic APC/C substrates

Deletion of *Apc2* in mice stabilizes securin and the cyclin substrates of the APC/C (Wirth et al., 2004). Reduction of the levels of APC2 in human cells was similarly shown to stabilize the early mitotic
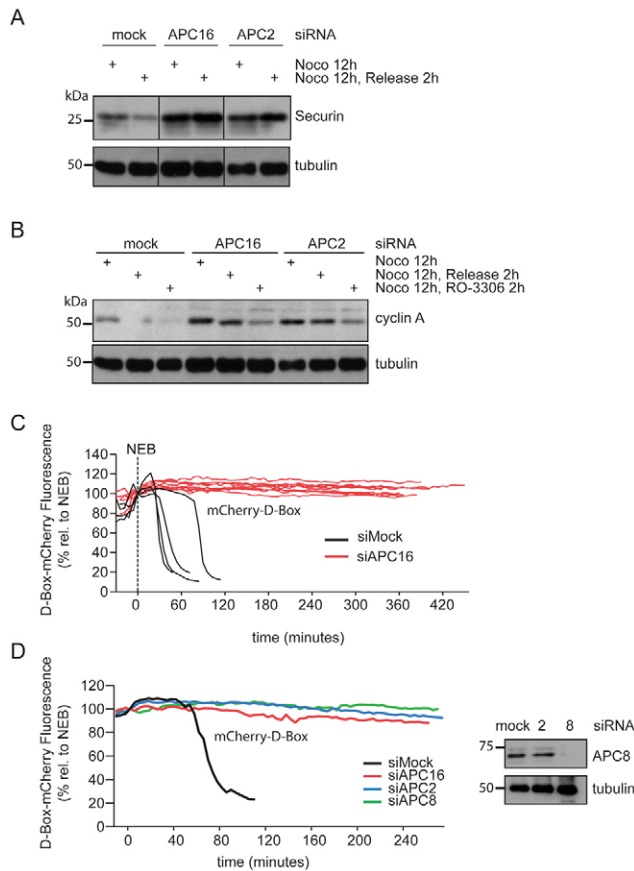
Fig. 3. Stabilization of APC/C substrates following depletion of APC16. (A,B) Immunoblots [securin and tubulin (A) or cyclin A and tubulin (B)] of lysates from HeLa cells transfected with the indicated siRNA oligonucleotides. In A, all cells were collected after 12 hours of nocodazole treatment or after an additional 2 hours following nocodazole washout. In B, mitotic APC/C siRNA cells were collected by shake-off prior to nocodazole addition, then treated with nocodazole for 12 hours followed by either nocodazole washout or treatment with the cdk1-inhibitor RO-3306 for an additional 2 hours. (C,D) Graph of relative fluorescence intensity of mCherry-D-Box (cyclin B$^{1-90}$) in individual HeLa-mCherry-cyclinB$^{1-90}$ cells transfected with the indicated siRNA oligonucleotides. In APC/C siRNA samples, only cells that were delayed in mitosis for at least 4 hours were analyzed for stability of mCherry-D-Box. Plots are representative of at least two independent experiments, at least five cells per experiment. Immunoblot in D shows APC8 and tubulin protein levels in the imaged cells.

APC/C substrate cyclin A (Wolthuis et al., 2008). To further determine whether APC16 plays a role in APC/C functionality, the levels of various substrates of the APC/C were examined in cells depleted of APC16, APC2 or APC8. Control populations were enriched for mitotic cells by treatment with nocodazole for 12 hours, after which the mitotic cells were harvested by shake-off. APC/C-subunit-depleted cells were first harvested by shake-off in the absence of nocodazole (to ensure enrichment of cells properly depleted of APC/C subunits; see Fig. 2C) and subsequently treated with nocodazole for 12 hours to allow comparison with mitotic control cells. Securin was easily detectable in nocodazole-treated control cells, and its levels diminished when cells were released from nocodazole and allowed to satisfy the mitotic checkpoint and initiate anaphase and mitotic exit (Fig. 3A). By contrast, Securin

levels in APC2- and APC16-depleted, nocodazole-treated cells were significantly higher than in controls and did not reduce upon nocodazole release (Fig. 3A). Although the latter is probably the result of the metaphase arrest of APC2- and APC16-depleted cells, the strikingly elevated securin levels in these cells after nocodazole treatment were indicative of a defect in APC/C activity. Normally, residual APC/C^{Cdc20} activity in cells treated with nocodazole is responsible for slow but persistent degradation of cyclin B in a process known as mitotic slippage (Brito and Rieder, 2006). The observations that securin is stabilized under similar circumstances upon depletion of APC16 or APC2 suggests that this residual APC/C activity is ablated in these cells.

As expected, nocodazole-treated control cells had low levels of the early mitotic APC/C substrate cyclin A (Wirth et al., 2004; Wolthuis et al., 2008) (Fig. 3B). The remaining pool of cyclin A in these cells was degraded upon release from nocodazole or after forced exit from mitosis by treatment with the Cdk1 inhibitor RO-3306 [Fig. 3B and Vassilev et al. (Vassilev et al., 2006)]. APC16- and APC2-depleted, nocodazole-treated cells, however, had high amounts of cyclin A, a significant fraction of which remained stable when these cells were forced out of mitosis (Fig. 3B). To measure APC/C-dependent protein destruction in real time (Clute and Pines, 1999), fluorescence of an artificial APC/C substrate was analyzed in HeLa cells stably expressing mCherry-cyclinB$^{1-90}$, containing the D-box of cyclin B, which is recognized and polyubiquitylated by the APC/C (Fang et al., 1998b; Gascoigne and Taylor, 2008). Total cellular fluorescence, set to 100% at nuclear envelope breakdown, remained relatively stable during the variable lengths of prometaphase in control cells, after which levels dropped to background within ~30 minutes at comparable rates (Fig. 3C,D). In cells depleted of APC16, mCherry-cyclinB$^{1-90}$ levels remained constant at or near 100% levels for several hours, showing no signs of slippage (Fig. 3C). Similarly, APC2- or APC8-depleted cells did not degrade mCherry-cyclinB$^{1-90}$ (Fig. 3D), indicating that APC/C activity was fully inhibited in cells depleted of any of the three APC/C subunits. Combined, these data strongly suggest that APC16 is a functional subunit of the APC/C that, like APC8 and the catalytic core subunit APC2, is of critical importance for APC/C activity towards mitotic substrates.

APC16 is not required for structural integrity of the APC/C holocomplex

A specific role within the APC/C complex has been ascribed to five of its twelve previously identified subunits in yeast and human cells (see Introduction for more details). In addition, there is interdependency of subunits with respect to incorporation into the APC/C. For example, the three TPR subunits in the 'head' region of the APC/C assemble in an ordered fashion: in yeast, APC6/Cdc16 is needed for binding of APC3/Cdc27, whereas APC8/Cdc23 is upstream of both other TPR subunits (Thornton et al., 2006). Deletion of APC13 in yeast prevents stable association of APC3/Cdc27 and APC6/Cdc16 with the APC/C holocomplex (Schwickart et al., 2004). Furthermore, deletion of Hcn1/Cdc26 in fission yeast causes disassembly of the APC/C into at least two subcomplexes, one containing the platform (APC1, 2, 4, 5 and 11) and one containing the other components (Yoon et al., 2006). The only report of a direct interactor of APC16 is the RING finger domain of Rb binding protein 6 (Chibi et al., 2008), suggesting APC16 may possibly interact with the APC11 RING finger.

To gather more insight into a potential role of APC16 in holocomplex assembly, we examined whether the APC/C was
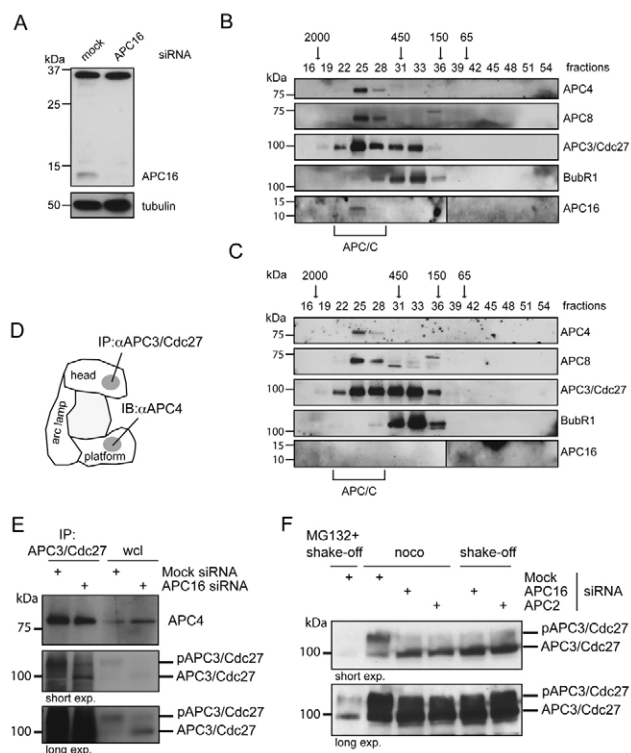
Fig. 4. APC16 is required for phosphorylation of APC3/Cdc27 but not for assembly of the APC/C holocomplex. (**A**) Immunoblots of whole cell lysates of the experiments shown in B and C. (**B,C**) Immunoblots of cellular fraction of (B) mock siRNA- or (C) APC16 siRNA-transfected HeLa cells after gel filtration. Migration of markers is indicated on top and the fractions containing APC/C are indicated at the bottom. Lines in the APC16 immunoblots indicate that the samples on either side were run on different gels. (**D**) Diagram of APC/C structure, according to Herzog et al. (Herzog et al., 2009). Approximate location of APC4 and APC3/Cdc27 are indicated. IP, immunoprecipitation. IB, immunoblot. (**E**) Immunoblots (APC3/Cdc27 and APC4) of anti-APC3/Cdc27 immunoprecipitates or whole cell lysates (wcl) from mitotic lysates of HeLa cells transfected with the indicated siRNA oligonucleotides. Mock siRNA-transfected cells were collected after 12 hours of nocodazole treatment, whereas APC16 siRNA-transfected cells were collected by mitotic shake-off. (**F**) Immunoblots (APC3/Cdc27) of whole cell lysates from mitotic HeLa cells transfected with the indicated siRNA oligonucleotides and left untreated (shake-off) or treated with nocodazole for 12 hours (noco) or MG132 for 90 minutes (MG132 + shake-off). Mock siRNA-transfected cells were treated with MG132 to enrich for mitotic cells in metaphase. Two chemiluminescence exposures (long and short exp.) are shown.

intact in cells lacking APC16. APC16-depleted cells (Fig. 4A) were collected by mitotic shake-off to ensure that only cells that had been properly depleted of APC16 were analyzed. APC/C composition was subsequently compared with that of mock-depleted cells by gelfiltration. In both mock- and APC16-depleted cells, the APC/C was comparable in size and contained at least APC3/Cdc27, APC4 and APC8 (Fig. 4B,C). In support of this, immunoprecipitation of the APC3/Cdc27 subunit within the head domain resulted in co-precipitation of the APC4 subunit within the platform in mock-transfected, nocodazole-treated cells (Fig. 4D). APC4 was similarly co-purified with APC3/Cdc27 in cells depleted of APC16 (Fig. 4D). Together, these experiments indicated that APC16, although essential for APC/C function, is not required for APC/C assembly and incorporation of at least APC3, 4, 5, 6, 8 and

13 into the APC/C holocomplex (Schwickart et al., 2004; Thornton et al., 2006).

We noted, however, that APC3/Cdc27 was hypophosphorylated in APC16-depleted cells. Although this hypophosphorylation might simply reflect a different phosphorylation state of metaphase APC/C [APC16 RNAi (Fig. 3B) or MG132 (Fig. 4E)] and prometaphase APC/C (nocodazole, Fig. 4E), we noted that prometaphase APC/C was similarly hypophosphorylated when APC2, 8 or 16 but not Cdc20 were depleted (Fig. 4E; supplementary material S2). Since Cdc20 siRNA nevertheless caused a profound delay in mitosis (supplementary material Fig. S2), this argues against APC/C activity in general, at least towards Cdc20-recognized targets, as a determinant of APC3/Cdc27 hyperphosphorylation. Together, these data show that APC16 is probably not involved in APC/C assembly and that APC16 is required for proper hyperphosphorylation of the APC3/Cdc27 subunit in prometaphase.

APC16 is functionally conserved in *Caenorhabditis elegans* and *Danio rerio*

Primary sequence alignment of human APC16 identified homologous sequences in the genomes of a variety of vertebrates (Fig. 5A; supplementary material Figs S3, S4). Sequence similarity was mostly in four patches, termed AH1-4 (for APC16 homology 1-4; Fig. 5B; supplementary material Fig. S3). The most significant similarity was found in AH4, suggesting this sequence is important for APC16 function. Based on this domain, homologues could be identified in a host of metazoans, including arthropods, nematodes, sponges, jellyfish and the simple multicellular organism trichoplax (supplementary material Figs S3, S4). Like APC7, however, no homologues could be identified in fungi including *S. pombe* or *S. cerevisiae*, but the genomes of various plants including *Arabidopsis thaliana* contain a possible APC16 homologue (Fig. 5A,B; supplementary material Figs S3, S4).

To examine whether some of these APC16-like proteins could be functional APC/C subunits, candidate orthologues in *C. elegans* (K10D2.4) or *D. rerio* (zgc:110659) were depleted by RNAi or morpholino oligonucleotides. Previous studies have shown that in *C. elegans* APC/C function is required for exit from meiotic M phase. Inhibition of various *C. elegans* APC/C subunits by RNAi or temperature-sensitive mutations causes a 'metaphase-to-anaphase-transition defective' (Mat) phenotype, which is highly characteristic for APC/C loss of function (Davis et al., 2002; Furuta et al., 2000; Golden et al., 2000). Importantly, knockdown of K10D2.4 by RNAi resulted in a clear Mat phenotype. Upon K10D2.4 RNAi, all fertilized eggs remained arrested at the one-cell stage within the hermaphrodite uterus (Fig. 5C). The arrest occurred at the metaphase-to-anaphase transition of meiosis I, and closely resembled depletion of *mat-2* (APC1) (Fig. 5C). In utero time-lapse microscopy of a K10D2.4-depleted fertilized egg showed the formation of a metaphase spindle, which persisted for the duration of the recording (67 minutes). By contrast, wild-type embryos initiated meiotic anaphase I after 5.1±0.89 minutes and anaphase II after 19.3±0.45 minutes following exit from the spermatheca (n=5; Fig. 5D,E; supplementary material Movies 1 and 2). The fact that inhibition of *C. elegans* K10D2.4 causes a highly specific APC/C loss-of-function phenotype indicates that K10D2.4 is an essential APC/C component and an orthologue of APC16.

Injection of ATG-directed morpholino oligonucleotides against APC/C subunits APC11 and APC16 into zebrafish embryos in both cases resulted in increased phospho-histone H3 staining in the
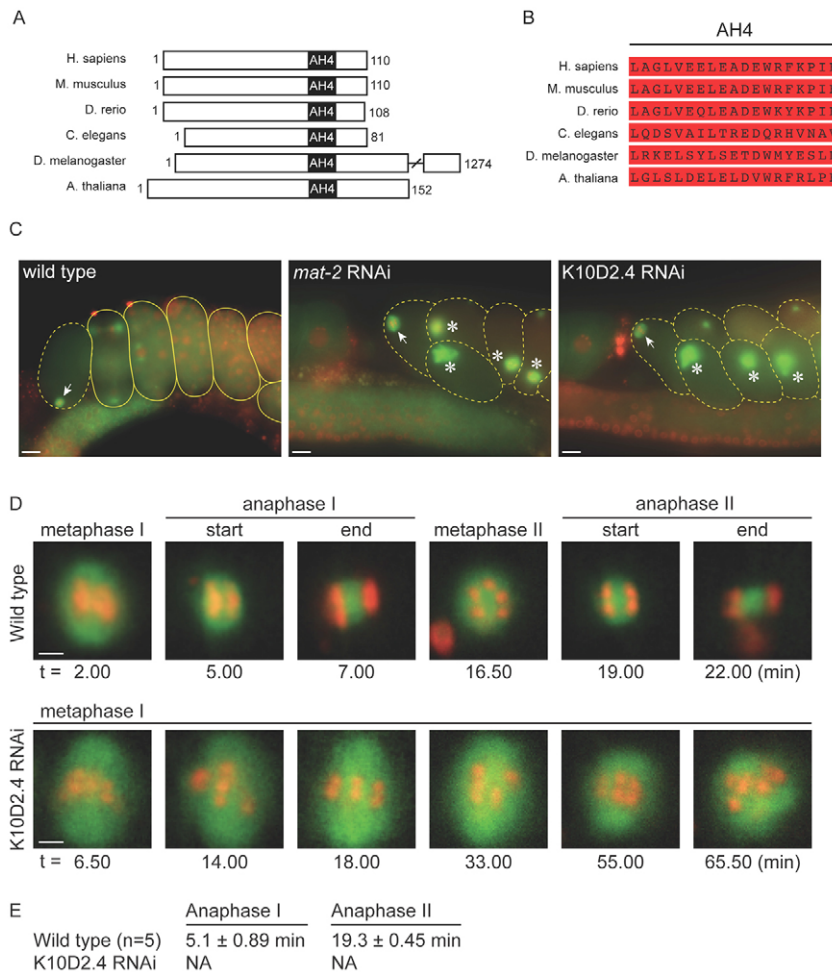
Fig. 5. K10D2.4 is a functional *C. elegans* orthologue of APC16. (**A**) Diagram of APC16-like protein sequences of the indicated organisms and the relative location of AH4 domain. (**B**) Sequence alignment of a part of the AH4 domain of the candidate APC16-like proteins. The *C. elegans* sequence is that of K10D2.4. GenBank entries for the corresponding nucleotide designated sequences are: NM_173473.2 (*H. sapiens*); BC025117.1 (*M. musculus*); NM_001017878.1 (*D. rerio*); NM_065697.4 (*C. elegans*); NM_139559.2 (*D. melanogaster*); NM_117569.2 (*A. thaliana*). (**C**) K10D2.4 knockdown results in a metaphase-arrest phenotype. *C. elegans* gonad showing embryos arrested at the one-cell stage (outlined) filling the uterus after K10D2.4 and *mat-2* RNAi. Arrows point to recently fertilized eggs with a metaphase spindle. Asterisks indicate spindles that have been in a prolonged metaphase arrest. Scale bars: 10 µm. Green, GFP–α-tubulin; red, mCherry–H2B. (**D**) Frames from time-lapse movies of meiotic spindles of a wild-type and K10D2.4 embryo. Exit from the spermatheca was taken as *t*=0. The cortex is to the left, background fluorescence was removed with the ImageJ 'subtract background' command. Scale bars: 2 µm. (**E**) Quantification of anaphase onset in wild-type and K10D2.4 RNAi embryos.

head region of the developing embryo (18-somite stage, 18 hours post-fertilization) when compared with control morpholino oligonucleotide injections (Fig. 6A-C). High magnification observation of the head region in knocked down embryos showed cells arrested in mitosis (Fig. 6C, inset) consistent with the delay in mitotic progression seen in cultured cells. Co-injection of mRNA coding for human APC16 fused at the C-terminus to EYFP (APC16^{EYFP}) rescued the increased pH3 staining in the head region (Fig. 6D). Quantification of pH3 staining (normalized to DAPI staining) in the head region showed more positive cells in APC11 and APC16 knocked down embryos compared with control embryos (Fig. 6E). This increase was rescued by human APC16^{EYFP} mRNA. Consistent with delayed mitotic progression increased apoptosis could be observed as early at the shield stage (6 hpf) in APC11 and APC16 knocked down embryos (Fig. 6F) that again was rescued with human APC16^{EYFP} mRNA. The increased mitotic index found in APC16 knocked down zebrafish embryos phenocopies the APC11 knockdown and is rescued by human APC16^{EYFP} mRNA. This supports the findings in human cells and worms showing that APC16 is a bona fide APC/C subunit responsible for timely mitotic progression.

Discussion

We have presented evidence that the 11.7 kDa protein C10orf104 (APC16) is a bona fide subunit of the APC/C. First, immunoprecipitations and gelfiltration showed that APC16 co-

purified and co-migrated with the APC/C and that APC16^{EYFP} coprecipitated E3 ubiquitin ligase activity. All recognized subunits of the APC/C are constitutively associated with the holocomplex (Kraft et al., 2003). Besides these, the APC/C interacts with many transient binding partners that do not constitute the core APC/C, including the coactivators, inhibitors and substrates. Our observations that APC16 co-purifies with the APC/C from both interphase and mitotic cells thus indicates that APC16 is likely a constitutive component of the APC/C. Second, APC16-depleted cells have profound delays at metaphase, and as such are indistinguishable from cells depleted of the recognized subunits APC2 and APC8. Third, the APC/C substrates cyclin A, securin and the D-box of cyclin B are stabilized in APC16-depleted cells. Again, for all three substrates, their levels and the duration of their stabilization upon APC16 depletion was similar to depletion of APC2 and APC8. Importantly, we have identified APC16 homologues throughout the animal and plant kingdoms and provide evidence of functional conservation of APC16 in the nematode *C. elegans* and the fish *D. rerio*. Thus, APC16 is probably essential for APC/C activity in all metazoans and plants.

It is unclear what the role of APC16 is within the APC/C. Unlike some other subunits, it is not required for APC/C assembly, and, although it is required for APC3/Cdc27 phosphorylation in prometaphase, this role is not unique to APC16. We are currently testing whether APC16 is involved in coactivator binding, substrate recognition or E2 binding. In conclusion, the metazoan APC/C has
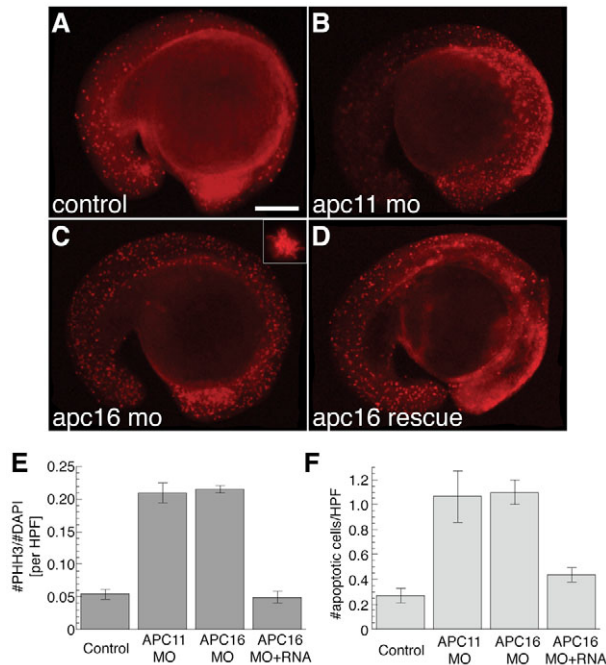
Fig. 6. zgc:110659 is a functional *D. rerio* orthologue of APC16.
(**A-D**) Larvae were stained in whole-mount for phospho-histone H3 (pH3, red) at the 18-somite stage. Lateral views of embryos show that many cells are pH3-positive in the head region of embryos in which APC11 (B) or APC16 (C) has been knocked down compared with (A) control larvae. Inset in C shows high power view of mitotically arrested cell in APC16 knocked down embryo. (D) APC16 knockdown is rescued by mRNA of human APC16 fused to EYFP. Scale bar: 200 μm. (**E,F**) A significant increase in (E) pH3-positive (normalized to DAPI-positive cells) and (F) apoptotic cells [per high power field (HPF)] was found in both APC11 and APC16 knocked down embryos and was rescued with human APC16[EYFP] mRNA.

a previously overlooked additional small subunit that is essential for its activity. APC16-like proteins were not identified in proteomics analyses of budding and fission yeast APC/C complexes (Yoon et al., 2002) and, similar to APC7, we were unable to recognize APC16 sequence orthologues in fungal genomes. It will be a future challenge to understand why metazoan and plant APC/C complexes may be composed of partly distinct subunits.

Materials and Methods
Plasmids
BubR1 was amplified by PCR from pcDNA3-myc-BubR1-ΔsiRNA (Kops et al., 2004) and inserted into the *Xho*I-*Bam*HI sites of pIC58 (pEYFP-LAP) to create pLAP-BubR1. LAP-BubR1 (AfeI-MfeI) was then transferred to pJag98 (*Sna*BI-*Eco*RI) to create pBabe-blast-LAP-BubR1. Mad2 was amplified by PCR from pJAG43 (EYFP-hsMad2) (Shah et al., 2004) and inserted into pJAG168 (pcDNA3.1, N-terminal TAP tag; protein A-TEV-CBP) to produce pcDNA3.1-TAP-Mad2 (pJAG179). TAP-Mad2 was excised from pJAG179 (*Pme*I) and inserted into pBABEpuro (*Sna*BI) to create pBABEpuro-TAP-Mad2 (pJAG184). APC16 was amplified by PCR from isolated HeLa cDNA (primers: 5′-ATGCATGCATAG-ATCTatggctgcttcatcatcatcc-3′, 5′-ATGCATGCATCTCGAGacctgaagagggggtgaatcc-3′) to permit cloning into EYFP-N1 (*Bgl*II-*Xho*I) or EYFP-C1 (*Bgl*II-*Xho*I). APC16 fusions to EYFP were cloned into pBABEblast (pJAG98) (*Afe*I-*Mfe*I into *Sna*BI-*Eco*RI) for generation of retrovirus. pLNCX2-mCherry-cyclinB[1-90] was a gift from Stephen Taylor (Gascoigne and Taylor, 2008). All sequences were verified by automated sequencing.

Cell lines, tissue culture and transfections
HeLa cells stably expressing LAP-BubR1, TAP-Mad2, APC16[EYFP] or mCherry-cyclinB[1-90] were established as described previously (Shah et al., 2004). In short, retrovirus of pLNCX2-mCherry-cyclinB[1-90], pBABEpuro-TAP-Mad2, or pBabe-

Blast-LAP-BubR1 or -APC16[EYFP] was produced from 293-GP cells and used to infect HeLa cells. After 2 weeks of selection with G418 (400 μg/ml; Sigma), puromycin (2 μg/ml; Sigma) or blasticidin (2 μg/ml; Sigma), either polyclonal lines were maintained (mCherry-cyclinB[1-90]) or single cells clones were selected by flow cytometry and analyzed for EYFP expression (BubR1, APC16) or TAP-expression (Mad2). HeLa cells and HeLa cell clones (H2B[EYFP], APC16[EYFP], mCherry-cyclinB[1-90], LAP-BubR1 or TAP-Mad2) were grown in DMEM with 8% FBS, supplemented with penicillin and streptomycin. Effectene (Qiagen) was used for plasmid transfections. Thymidine (2 mM), aphidicolin (5 μg/ml) and nocodazole (200 ng ml^{-1}) were from Sigma. RO-3306 (10 μM) was purchased from EMD Biosciences.

Short interfering RNAs
siRNAs to APC16 (C10orf104) were purchased from Dharmacon (siRNA 9, 11, 12: LQ-018378-01) and Qiagen (siRNA 7: SI04267564). siRNAs to Mock (5′-AGA-UUCUAGCUAACUGUUC-3′), APC8 (L-009523-00) and APC2 (J-003200-13) were from Dharmacon. siRNA transfections were done using HiPerfect (Qiagen) and according to the thymidine-aphidicolin protocol of Meraldi et al. (Meraldi et al., 2004). In short, cells were blocked with thymidine (2 mM) for 16 hours, released into medium for 6 hours and transfected with siRNA oligonucleotides. Three hours post-transfection, aphidicolin (5 μg/ml) was added for 24 hours and released into medium with or without spindle poisons and prepared for further analysis 12 hours after release.

Tandem-affinity purifications and mass spectrometry
10[12] or 10[13] cells of HeLa-LAP-BubR1 or HeLa-TAP-Mad2 clones, respectively (see Fig. 1), were blocked in 300 nM nocodazole for 16 hours. Cells were collected and mixed for further purification of native complexes as described previously (Cheeseman and Desai, 2005). Mass spectrometry was conducted essentially as described by Cheeseman et al. (Cheeseman et al., 2004). The samples were analyzed using a ThermoFinnigan LTQ mass spectrometer using Mudpit with the following gradients of 500 mM ammonium acetate: 10, 25, 35, 50, 65, 80 and 100%. Results were searched by Sequest against an NCBI human-mouse-rat database and filtered with DTA Select.

Antibodies, immunoprecipitations, immunoblotting and silver stains
A polyclonal antibody to APC16 was prepared from rabbits using a fast immunization protocol (Davids Biotech, Germany). Rabbits were injected with a mixture of peptides (SDLAPPRKALFTYPKGAG, ASTLKQVKHDQQVARMEKLA, and LEADEWRFKPIEQLLGFTPSSG), and antibody was affinity purified against this mixture. Rabbit anti-GFP was a custom polyclonal antibody. Sheep anti-BubR1 was a custom polyclonal antibody, produced according to the methods of Taylor et al. (Taylor et al., 2001). Other antibodies used were, mouse anti-Cdc27 (for immunoblots; BD Transduction Labs), rabbit anti-Cdc27 (for immunoprecipitations; a gift from P. Hieter), goat anti-APC4 (C-18; Santa Cruz Biotechnology), rabbit anti-APC8 (A301-181A), rabbit anti-PTTG (Securin, Zymed), rabbit anti-cyclin A (H-432; Santa Cruz Biotechnology) and mouse anti-α-tubulin (Sigma). Secondary antibodies for immunoblotting were from Bio-Rad. For immunoprecipitations, cells were lysed (50 mM Tris pH 7.5, 150 mM NaCl₂, 1% Trition X-100, 5 mM EDTA, 1 mM Na₃VO₄, 1 mM β-glycerophosphate, 1 mM NaF and complete protease inhibitor cocktail; Roche), cleared by centrifugation at 21,000 *g* for 5 minutes, and incubated with antibodies coupled to protein A agarose for 2 hours at 4°C. Precipitates were washed four times with lysis buffer and prepared for further analysis. SDS-PAGE electrophoresis and immunoblotting were performed according to standard procedures. Silver staining was done by fixing the gel twice for 15 minutes with 30% ethanol/10% acetic acid followed by a 30-minute incubation in 0.1 g Na₂S₂O₃, 30% ethanol, 2.5 ml 4 M sodium acetate (pH 6.8). Gels were washed thoroughly with water and incubated with 0.1 g AgNO₃, 25 ml CH₂O (formaldehyde) for 30 minutes and developed with 2.5 g Na₂CO₃, 50 ml CH₂O. The reaction was stopped with 1% acetic acid.

APC/C ubiquitylation assay
Functional APC/C was purified from mitotic wild-type HeLa cell extracts or from mitotic APC16[EYFP] HeLa cell extracts as described by Reddy and colleagues (Reddy et al., 2007). Anti-GFP (Abcam)-bound Protein G beads were incubated with mitotic (checkpoint) HeLa APC16[EYFP] extracts. In vitro ubiquitylation assays were carried out as previously described (Rape and Kirschner, 2004) with HA-ubiquitin (Boston Biochem) in place of ubiquitin. Recombinant securin was kindly provided by Tao Wu (Harvard Medical School). Substrate ubiquitylation was detected using immunoblotting using anti-HA antibody (Abcam).

Gel filtration
Cells were lysed (50 mM Tris pH 7.5, 150 mM NaCl₂, 1% Trition X-100, 5 mM EDTA, 2 mM MgCl₂, 1 mM Na₃VO₄, 1 mM β-glycerophosphate, 1 mM NaF and complete protease inhibitor cocktail; Roche), cleared by centrifugation at 21,000 *g* for 10 minutes, and set to a protein concentration of 10 mg/ml. Lysates were separated on a Superose 6 HR10/30 column (Pharmacia) at a flow rate of 0.25 ml/min in lysis buffer without protease inhibitors, and 400 μl fractions were collected.

Live-cell microscopy

For live-cell imaging, cells were plated in eight-well chambered glass-bottom slides (LabTek II) or 24-well glass bottom plates (MatTek), transfected and imaged in a heated chamber (37°C and 5% CO_2) using a ×20/0.5 NA UPLFLN objective on a Olympus IX-81 microscope, controlled by Cell-M software (Olympus). 16 bit DIC, EYFP or mCherry fluorescence images were acquired every 4 minutes using a Hamamatsu ORCA-ER camera. Images of H2B-eYFP are maximum intensity projections of all Z-planes and were processed using Cell-M software. mCherry-CyclinB[1-90] signal intensities were quantified with ImageJ software. Circumferences of cells were drawn and average intensities over time were corrected for bleaching and background, related to area and plotted relative to the value at nuclear envelope breakdown (100%).

C. elegans studies

Caenorhabditis elegans strains were maintained as described previously (Sulston and Brenner, 1974). The strain used in this study was SV1010 [*ruIs57(unc-119*(+) *pie-1*-GFP-α-tubulin); *itIs37(unc-119*(+) *pie-1*-mCherry–H2B)] (may contain unc-119 (eds) III)], which was created by crossing strain EU1561 with strain AZ244. The RNAi clone for K10D2.4 was obtained from the Ahringer RNAi library (Kamath et al., 2003). For dsRNA production, gene fragments were amplified in PCR reactions with flanking T7 primers, followed by in vitro transcription with an Ambion MegaScript transcription kit. To obtain knockdown by RNAi, double-stranded RNA was injected into the gonad of young adult hermaphrodites (Fire et al., 1998). After injection, animals were kept at 25°C for 24 hours before in vivo imaging. For in utero time-lapse recordings, gravid hermaphrodites were anaesthetized for 30 minutes in M9 medium containing 0.1% tricaine and 0.01% tetramisole on 2% agarose pads. Time-lapse recordings were performed at 20°C. Wide-field fluorescence and differential interference contrast (DIC) movies were recorded at 30-second intervals with a ×100/1.4 NA PlanApochromat objective lens with 400 msecond exposures on a motorized microscope (Zeiss Axioplan). Fluorescence excitation light was filtered to 10% transmission with neutral density filters, and binning was set to 2×2 with automatic gain adjustments.

Zebrafish studies

Maintenance and breeding of zebrafish (*Danio rerio*) were carried out according to standard protocols. Wild-type embryos of AB fish were injected with 375 μM Apc16 (5′-ATCTGGCGCATCTAGGACTTACCCG-3′) or Apc11 (5′-ACCTTCATTCC-TTTGTTACGTTCTC-3′) morpholino oligonucleotides targeting the ATG site or a control morpholino oligonucleotide (5′-CCTCTTACCTCAGTTACAATTTATA-3′). Three independent trials were performed with embryos derived from different parents and injected on different days. The coding sequence of human APC16 fused at the C-terminus to EYFP was cloned into pCS2+. This clone was used to generate sense mRNA using the Ambion SP6 mMessage Machine kit. For rescue experiments, 20 pg of human APC16-EYFP mRNA in Tris-EDTA (TE) were co-injected with the morpholino oligonucleotides into the embryo at the one- to two-cell stage. Whole-mount immunohistochemistry was carried out as previously described (Wehman et al., 2005). Briefly, larvae at the shield stage (6 hours post-fertilization; hpf) and 18-somite stages (18 hpf) were fixed in 4% paraformaldehyde (PFA) in phosphate-buffered saline (PBS), dehydrated in methanol and stored at –20°C. Larvae were then rehydrated and digested with 5 μg/ml proteinase K for 10 minutes. Embryos were stained with rabbit anti-phospho-histone H3 (PHH3) antibody (1:1000, Sigma) followed by goat anti-rabbit-Cy3 (1:400, Jackson Laboratories). Embryos were then co-stained with DAPI. To examine apoptotic cell death, larvae were stained at shield stage with Acridine Orange (Langheinrich et al., 2002). Whole-mount images were taken at ×4 and high power fields were imaged at ×100.

Note added in proof

We call your attention to a recent paper that also identified APC16 as a subunit of the APC/C in human cells (Hutchins et al., 2010).
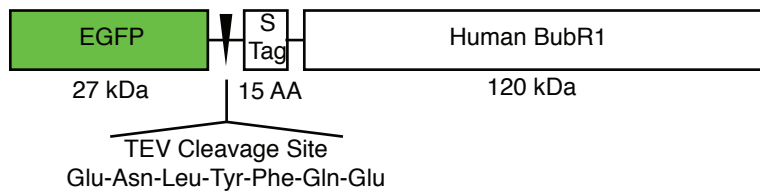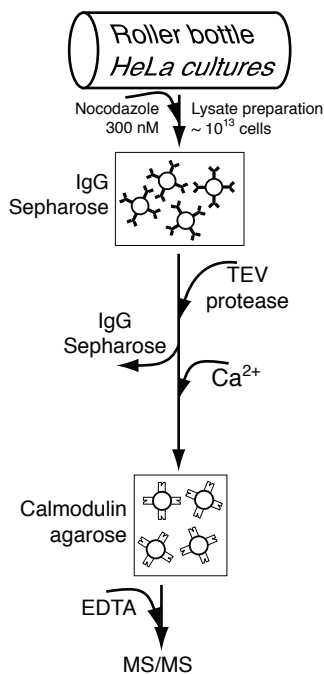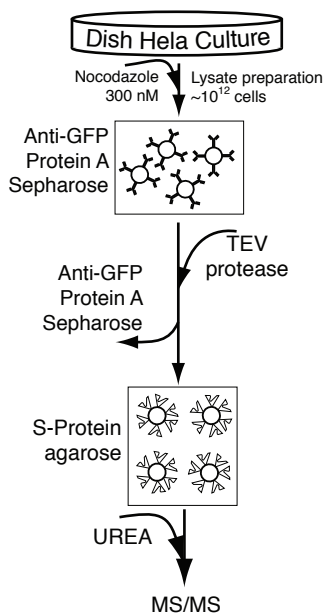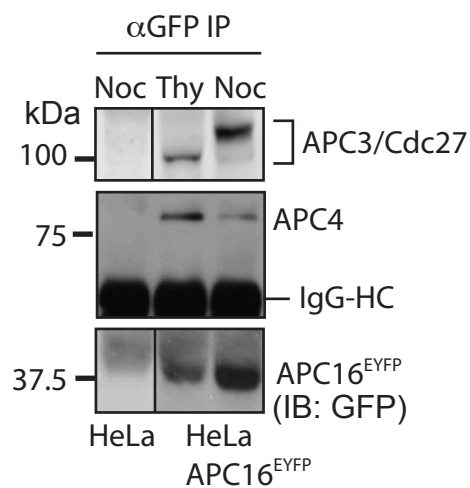
References

Aristarkhov, A., Eytan, E., Moghe, A., Admon, A., Hershko, A. and Ruderman, J. V. (1996). E2-C, a cyclin-selective ubiquitin carrier protein required for the destruction of mitotic cyclins. *Proc. Natl. Acad. Sci. USA* **93**, 4294-4299.

Brito, D. A. and Rieder, C. L. (2006). Mitotic checkpoint slippage in humans occurs via cyclin B destruction in the presence of an active checkpoint. *Curr. Biol.* **16**, 1194-1200.

Burton, J. L. and Solomon, M. J. (2007). Mad3p, a pseudosubstrate inhibitor of APCCdc20 in the spindle assembly checkpoint. *Genes Dev.* **21**, 655-667.

Capron, A., Okresz, L. and Genschik, P. (2003). First glance at the plant APC/C, a highly conserved ubiquitin-protein ligase. *Trends Plant Sci.* **8**, 83-89.

Carroll, C. W. and Morgan, D. O. (2002). The Doc1 subunit is a processivity factor for the anaphase-promoting complex. *Nat. Cell. Biol.* **4**, 880-887.

Cheeseman, I. M. and Desai, A. (2005). A combined approach for the localization and tandem affinity purification of protein complexes from metazoans. *Sci STKE* **2005**, pl1.

Cheeseman, I. M., Niessen, S., Anderson, S., Hyndman, F., Yates, J. R., 3rd, Oegema, K. and Desai, A. (2004). A conserved protein network controls assembly of the outer kinetochore and its ability to sustain tension. *Genes Dev.* **18**, 2255-2268.

Chen, R. H., Shevchenko, A., Mann, M. and Murray, A. W. (1998). Spindle checkpoint protein Xmad1 recruits Xmad2 to unattached kinetochores. *J. Cell Biol.* **143**, 283-295.

Chibi, M., Meyer, M., Skepu, A., Rees, D. J. G., Moolman-Smook, J. C. and Pugh, D. J. R. (2008). RBBP6 interacts with multifunctional protein YB-1 through its RING finger domain, leading to ubiquitination and proteosomal degradation of YB-1. *J. Mol. Biol.* **384**, 908-916.

Clute, P. and Pines, J. (1999). Temporal and spatial control of cyclin B1 destruction in metaphase. *Nat. Cell. Biol.* **1**, 82-87.

Cohen-Fix, O., Peters, J. M., Kirschner, M. W. and Koshland, D. (1996). Anaphase initiation in Saccharomyces cerevisiae is controlled by the APC-dependent degradation of the anaphase inhibitor Pds1p. *Genes Dev.* **10**, 3081-3093.

Cui, X. Y., Chen, J. X., Liu, B. W., Xiao, L. Y. and Fang, D. Z. (2009). Identification of a novel gene, MSAG, regulated by high levels of glucose and insulin. *Biochemistry (Mosc.)* **74**, 22-28.

Davis, E. S., Wille, L., Chestnut, B. A., Sadler, P. L., Shakes, D. C. and Golden, A. (2002). Multiple subunits of the Caenorhabditis elegans anaphase-promoting complex are required for chromosome segregation during meiosis I. *Genetics* **160**, 805-813.

De Antoni, A., Pearson, C. G., Cimini, D., Canman, J. C., Sala, V., Nezi, L., Mapelli, M., Sironi, L., Faretta, M., Salmon, E. D. et al. (2005). The Mad1/Mad2 complex as a template for Mad2 activation in the spindle assembly checkpoint. *Curr. Biol.* **15**, 214-225.

den Elzen, N. and Pines, J. (2001). Cyclin A is destroyed in prometaphase and can delay chromosome alignment and anaphase. *J. Cell Biol.* **153**, 121-136.

Fang, G. (2002). Checkpoint protein BubR1 acts synergistically with Mad2 to inhibit anaphase-promoting complex. *Mol. Biol. Cell* **13**, 755-766.

Fang, G., Yu, H. and Kirschner, M. W. (1998a). The checkpoint protein MAD2 and the mitotic regulator CDC20 form a ternary complex with the anaphase-promoting complex to control anaphase initiation. *Genes Dev.* **12**, 1871-1883.

Fang, G., Yu, H. and Kirschner, M. W. (1998b). Direct binding of CDC20 protein family members activates the anaphase-promoting complex in mitosis and G1. *Mol. Cell* **2**, 163-171.

Fire, A., Xu, S., Montgomery, M. K., Kostas, S. A., Driver, S. E. and Mello, C. C. (1998). Potent and specific genetic interference by double-stranded RNA in Caenorhabditis elegans. *Nature* **391**, 806-811.

Funabiki, H. and Murray, A. W. (2000). The Xenopus chromokinesin Xkid is essential for metaphase chromosome alignment and must be degraded to allow anaphase chromosome movement. *Cell* **102**, 411-424.

Funabiki, H., Yamano, H., Kumada, K., Nagao, K., Hunt, T. and Yanagida, M. (1996). Cut2 proteolysis required for sister-chromatid seperation in fission yeast. *Nature* **381**, 438-441.

Furuta, T., Tuck, S., Kirchner, J., Koch, B., Auty, R., Kitagawa, R., Rose, A. M. and Greenstein, D. (2000). EMB-30: an APC4 homologue required for metaphase-to-anaphase transitions during meiosis and mitosis in Caenorhabditis elegans. *Mol. Biol. Cell* **11**, 1401-1419.

Gabellini, D., Colaluca, I. N., Vodermaier, H. C., Biamonti, G., Giacca, M., Falaschi, A., Riva, S. and Peverali, F. A. (2003). Early mitotic degradation of the homeoprotein HOXC10 is potentially linked to cell cycle progression. *EMBO J.* **22**, 3715-3724.

Garnett, M. J., Mansfeld, J., Godwin, C., Matsusaka, T., Wu, J., Russell, P., Pines, J. and Venkitaraman, A. R. (2009). UBE2S elongates ubiquitin chains on APC/C substrates to promote mitotic exit. *Nat. Cell. Biol.* **11**, 1363-1369.

Gascoigne, K. E. and Taylor, S. S. (2008). Cancer cells display profound intra- and interline variation following prolonged exposure to antimitotic drugs. *Cancer Cell* **14**, 111-122.

Geley, S., Kramer, E., Gieffers, C., Gannon, J., Peters, J. M. and Hunt, T. (2001). Anaphase-promoting complex/cyclosome-dependent proteolysis of human cyclin A starts at the beginning of mitosis and is not subject to the spindle assembly checkpoint. *J. Cell Biol.* **153**, 137-148.

Gmachl, M., Gieffers, C., Podtelejnikov, A. V., Mann, M. and Peters, J. M. (2000). The RING-H2 finger protein APC11 and the E2 enzyme UBC4 are sufficient to ubiquitinate substrates of the anaphase-promoting complex. *Proc. Natl. Acad. Sci. USA* **97**, 8973-8978.

Golden, A., Sadler, P. L., Wallenfang, M. R., Schumacher, J. M., Hamill, D. R., Bates, G., Bowerman, B., Seydoux, G. and Shakes, D. C. (2000). Metaphase to anaphase (mat) transition-defective mutants in Caenorhabditis elegans. *J. Cell Biol.* **151**, 1469-1482.

Habu, T., Kim, S. H., Weinstein, J. and Matsumoto, T. (2002). Identification of a MAD2-binding protein, CMT2, and its role in mitosis. *EMBO J.* **21**, 6419-6428.

Hagting, A., Den Elzen, N., Vodermaier, H. C., Waizenegger, I. C., Peters, J. M. and Pines, J. (2002). Human securin proteolysis is controlled by the spindle checkpoint and reveals when the APC/C switches from activation by Cdc20 to Cdh1. *J. Cell Biol.* **157**, 1125-1137.

Hames, R. S., Wattam, S. L., Yamano, H., Bacchieri, R. and Fry, A. M. (2001). APC/C-mediated destruction of the centrosomal kinase Nek2A occurs in early mitosis and depends upon a cyclin A-type D-box. *EMBO J.* **20**, 7117-7127.

Hardwick, K. G., Johnston, R. C., Smith, D. L. and Murray, A. W. (2000). MAD3 encodes a novel component of the spindle checkpoint which interacts with Bub3p, Cdc20p, and Mad2p. *J. Cell Biol.* **148**, 871-882.

Hartwell, L. H., Culotti, J., Pringle, J. R. and Reid, B. J. (1974). Genetic control of the cell division cycle in yeast. *Science* **183**, 46-51.

Herzog, F., Primorac, I., Dube, P., Lenart, P., Sander, B., Mechtler, K., Stark, H. and Peters, J. M. (2009). Structure of the anaphase-promoting complex/cyclosome interacting with a mitotic checkpoint complex. *Science* **323**, 1477-1481.

Hutchins, J. R., Toyoda, Y., Hegemann, B., Poser, I., Hériché, J. K., Sykora, M. M., Augsburg, M., Hudecz, O., Buschhorn, B. A., Bulkescher, J. et al. (2010). Systematic analysis of human protein complexes identifies chromosome segregation proteins. *Science* DOI: 10.1126/science.1181348.

Irniger, S., Piatti, S., Michaelis, C. and Nasmyth, K. (1995). Genes involved in sister chromatid separation are needed for B-type cyclin proteolysis in budding yeast. *Cell* **81**, 269-278.

Kamath, R. S., Fraser, A. G., Dong, Y., Poulin, G., Durbin, R., Gotta, M., Kanapin, A., Le Bot, N., Moreno, S., Sohrmann, M. et al. (2003). Systematic functional analysis of the Caenorhabditis elegans genome using RNAi. *Nature* **421**, 231-237.

King, E. M., van der Sar, S. J. and Hardwick, K. G. (2007). Mad3 KEN boxes mediate both Cdc20 and Mad3 turnover, and are critical for the spindle checkpoint. *PLoS One* **2**, e342.

King, R. W., Peters, J. M., Tugendreich, S., Rolfe, M., Hieter, P. and Kirschner, M. W. (1995). A 20S complex containing CDC27 and CDC16 catalyzes the mitosis-specific conjugation of ubiquitin to cyclin B. *Cell* **81**, 279-288.

Kiyomitsu, T., Obuse, C. and Yanagida, M. (2007). Human Blinkin/AF15q14 is required for chromosome alignment and the mitotic checkpoint through direct interaction with Bub1 and BubR1. *Dev. Cell* **13**, 663-676.

Kops, G. J., Foltz, D. R. and Cleveland, D. W. (2004). Lethality to human cancer cells through massive chromosome loss by inhibition of the mitotic checkpoint. *Proc. Natl. Acad. Sci. USA* **101**, 8699-8704.

Kraft, C., Herzog, F., Gieffers, C., Mechtler, K., Hagting, A., Pines, J. and Peters, J. M. (2003). Mitotic regulation of the human anaphase-promoting complex by phosphorylation. *EMBO J.* **22**, 6598-6609.

Kramer, E. R., Gieffers, C., Holzl, G., Hengstschlager, M. and Peters, J. M. (1998). Activation of the human anaphase-promoting complex by proteins of the CDC20/Fizzy family. *Curr. Biol.* **8**, 1207-1210.

Kulukian, A., Han, J. S. and Cleveland, D. W. (2009). Unattached kinetochores catalyze production of an anaphase inhibitor that requires a Mad2 template to prime Cdc20 for BubR1 binding. *Dev. Cell* **16**, 105-117.

Lamb, J. R., Michaud, W. A., Sikorski, R. S. and Hieter, P. A. (1994). Cdc16p, Cdc23p and Cdc27p form a complex essential for mitosis. *EMBO J.* **13**, 4321-4328.

Langheinrich, U., Hennen, E., Stott, G. and Vacun, G. (2002). Zebrafish as a model organism for the identification and characterization of drugs and genes affecting p53 signaling. *Curr. Biol.* **12**, 2023-2028.

Lee, S. H., Sterling, H., Burlingame, A. and McCormick, F. (2008). Tpr directly binds to Mad1 and Mad2 and is important for the Mad1-Mad2-mediated mitotic spindle checkpoint. *Genes Dev.* **22**, 2926-2931.

Leverson, J. D., Joazeiro, C. A., Page, A. M., Huang, H., Hieter, P. and Hunter, T. (2000). The APC11 RING-H2 finger mediates E2-dependent ubiquitination. *Mol. Biol. Cell* **11**, 2315-2325.

Li, M. and Zhang, P. (2009). The function of APC/CCdh1 in cell cycle and beyond. *Cell Div.* **4**, 2.

Lindon, C. and Pines, J. (2004). Ordered proteolysis in anaphase inactivates Plk1 to contribute to proper mitotic exit in human cells. *J. Cell Biol.* **164**, 233-241.

Malureanu, L. A., Jeganathan, K. B., Hamada, M., Wasilewski, L., Davenport, J. and van Deursen, J. M. (2009). BubR1 N terminus acts as a soluble inhibitor of cyclin B degradation by APC/C(Cdc20) in interphase. *Dev. Cell* **16**, 118-131.

Matyskiela, M. E. and Morgan, D. O. (2009). Analysis of activator-binding sites on the APC/C supports a cooperative substrate-binding mechanism. *Mol. Cell* **34**, 68-80.

McGarry, T. J. and Kirschner, M. W. (1998). Geminin, an inhibitor of DNA replication, is degraded during mitosis. *Cell* **93**, 1043-1053.

Meraldi, P., Draviam, V. M. and Sorger, P. K. (2004). Timing and checkpoints in the regulation of mitotic progression. *Dev. Cell* **7**, 45-60.

Montembault, E., Dutertre, S., Prigent, C. and Giet, R. (2007). PRP4 is a spindle assembly checkpoint protein required for MPS1, MAD1, and MAD2 localization to the kinetochores. *J. Cell Biol.* **179**, 601-609.

Musacchio, A. and Salmon, E. D. (2007). The spindle-assembly checkpoint in space and time. *Nat. Rev. Mol. Cell. Biol.* **8**, 379-393.

Nilsson, J., Yekezare, M., Minshull, J. and Pines, J. (2008). The APC/C maintains the spindle assembly checkpoint by targeting Cdc20 for destruction. *Nat. Cell. Biol.* **10**, 1411-1420.

Osaka, F., Seino, H., Seno, T. and Yamao, F. (1997). A ubiquitin-conjugating enzyme in fission yeast that is essential for the onset of anaphase in mitosis. *Mol. Cell. Biol.* **17**, 3388-3397.

Page, A. M., Aneliunas, V., Lamb, J. R. and Hieter, P. (2005). In vivo characterization of the nonessential budding yeast anaphase-promoting complex/cyclosome components Swm1p, Mnd2p and Apc9p. *Genetics* **170**, 1045-1062.

Palframan, W. J., Meehl, J. B., Jaspersen, S. L., Winey, M. and Murray, A. W. (2006). Anaphase inactivation of the spindle checkpoint. *Science* **313**, 680-684.

Passmore, L. A., McCormack, E. A., Au, S. W., Paul, A., Willison, K. R., Harper, J. W. and Barford, D. (2003). Doc1 mediates the activity of the anaphase-promoting complex by contributing to substrate recognition. *EMBO J.* **22**, 786-796.

Peters, J. M. (2006). The anaphase promoting complex/cyclosome: a machine designed to destroy. *Nat. Rev. Mol. Cell. Biol.* **7**, 644-656.

Pfleger, C. M. and Kirschner, M. W. (2000). The KEN box: an APC recognition signal distinct from the D box targeted by Cdh1. *Genes Dev.* **14**, 655-665.

Poser, I., Sarov, M., Hutchins, J. R., Heriche, J. K., Toyoda, Y., Pozniakovsky, A., Weigl, D., Nitzsche, A., Hegemann, B., Bird, A. W. et al. (2008). BAC TransgeneOmics: a high-throughput method for exploration of protein function in mammals. *Nat. Methods* **5**, 409-415.

Prinz, S., Hwang, E. S., Visintin, R. and Amon, A. (1998). The regulation of Cdc20 proteolysis reveals a role for APC components Cdc23 and Cdc27 during S phase and early mitosis. *Curr. Biol.* **8**, 750-760.

Rape, M. and Kirschner, M. W. (2004). Autonomous regulation of the anaphase-promoting complex couples mitosis to S-phase entry. *Nature* **432**, 588-595.

Reddy, S. K., Rape, M., Margansky, W. A. and Kirschner, M. W. (2007). Ubiquitination by the anaphase-promoting complex drives spindle checkpoint inactivation. *Nature* **446**, 921-925.

Schwickart, M., Havlis, J., Habermann, B., Bogdanova, A., Camasses, A., Oelschlaegel, T., Shevchenko, A. and Zachariae, W. (2004). Swm1/Apc13 is an evolutionarily conserved subunit of the anaphase-promoting complex stabilizing the association of Cdc16 and Cdc27. *Mol. Cell. Biol.* **24**, 3562-3576.

Shah, J. V., Botvinick, E., Bonday, Z., Furnari, F., Berns, M. and Cleveland, D. W. (2004). Dynamics of centromere and kinetochore proteins; implications for checkpoint signaling and silencing. *Curr. Biol.* **14**, 942-952.

Sigrist, S. J. and Lehner, C. F. (1997). Drosophila fizzy-related down-regulates mitotic cyclins and is required for cell proliferation arrest and entry into endocycles. *Cell* **90**, 671-681.

Stewart, S. and Fang, G. (2005). Destruction box-dependent degradation of aurora B is mediated by the anaphase-promoting complex/cyclosome and Cdh1. *Cancer Res.* **65**, 8730-8735.

Sudakin, V., Ganoth, D., Dahan, A., Heller, H., Hershko, J., Luca, F. C., Ruderman, J. V. and Hershko, A. (1995). The cyclosome, a large complex containing cyclin-selective ubiquitin ligase activity, targets cyclins for destruction at the end of mitosis. *Mol. Biol. Cell* **6**, 185-197.

Sudakin, V., Chan, G. K. and Yen, T. J. (2001). Checkpoint inhibition of the APC/C in HeLa cells is mediated by a complex of BUBR1, BUB3, CDC20, and MAD2. *J. Cell Biol.* **154**, 925-936.

Sulston, J. E. and Brenner, S. (1974). The DNA of Caenorhabditis elegans. *Genetics* **77**, 95-104.

Tang, Z., Bharadwaj, R., Li, B. and Yu, H. (2001a). Mad2-Independent inhibition of APCCdc20 by the mitotic checkpoint protein BubR1. *Dev. Cell* **1**, 227-237.

Tang, Z., Li, B., Bharadwaj, R., Zhu, H., Ozkan, E., Hakala, K., Deisenhofer, J. and Yu, H. (2001b). APC2 Cullin protein and APC11 RING protein comprise the minimal ubiquitin ligase module of the anaphase-promoting complex. *Mol. Biol. Cell* **12**, 3839-3851.

Taylor, S. S., Hussein, D., Wang, Y., Elderkin, S. and Morrow, C. J. (2001). Kinetochore localisation and phosphorylation of the mitotic checkpoint components Bub1 and BubR1 are differentially regulated by spindle events in human cells. *J. Cell Sci.* **114**, 4385-4395.

Thornton, B. R. and Toczyski, D. P. (2003). Securin and B-cyclin/CDK are the only essential targets of the APC. *Nat. Cell. Biol.* **5**, 1090-1094.

Thornton, B. R., Ng, T. M., Matyskiela, M. E., Carroll, C. W., Morgan, D. O. and Toczyski, D. P. (2006). An architectural map of the anaphase-promoting complex. *Genes Dev* **20**, 449-460.

Townsley, F. M., Aristarkhov, A., Beck, S., Hershko, A. and Ruderman, J. V. (1997). Dominant-negative cyclin-selective ubiquitin carrier protein E2-C/UbcH10 blocks cells in metaphase. *Proc. Natl. Acad. Sci. USA* **94**, 2362-2367.

Tugendreich, S., Tomkiel, J., Earnshaw, W. and Hieter, P. (1995). CDC27Hs colocalizes with CDC16Hs to the centrosome and mitotic spindle and is essential for the metaphase to anaphase transition. *Cell* **81**, 261-268.

Vassilev, L. T., Tovar, C., Chen, S., Knezevic, D., Zhao, X., Sun, H., Heimbrook, D. C. and Chen, L. (2006). Selective small-molecule inhibitor reveals critical mitotic functions of human CDK1. *Proc. Natl. Acad. Sci. USA* **103**, 10660-10665.

Visintin, R., Prinz, S. and Amon, A. (1997). CDC20 and CDH1: a family of substrate-specific activators of APC-dependent proteolysis. *Science* **278**, 460-463.

Vodermaier, H. C., Gieffers, C., Maurer-Stroh, S., Eisenhaber, F. and Peters, J. M. (2003). TPR subunits of the anaphase-promoting complex mediate binding to the activator protein CDH1. *Curr. Biol.* **13**, 1459-1468.

Walker, A., Acquaviva, C., Matsusaka, T., Koop, L. and Pines, J. (2008). UbcH10 has a rate-limiting role in G1 phase but might not act in the spindle checkpoint or as part of an autonomous oscillator. *J. Cell Sci.* **121**, 2319-2326.

Wehman, A. M., Staub, W., Meyers, J. R., Raymond, P. A. and Baier, H. (2005). Genetic dissection of the zebrafish retinal stem-cell compartment. *Dev. Biol.* **281**, 53-65.

Williamson, A., Wickliffe, K. E., Mellone, B. G., Song, L., Karpen, G. H. and Rape, M. (2009). Identification of a physiological E2 module for the human anaphase-promoting complex. *Proc. Natl. Acad. Sci. USA* **106**, 18213-18218.

Wirth, K. G., Ricci, R., Gimenez-Abian, J. F., Taghybeeglu, S., Kudo, N. R., Jochum, W., Vasseur-Cognet, M. and Nasmyth, K. (2004). Loss of the anaphase-promoting complex in quiescent cells causes unscheduled hepatocyte proliferation. *Genes Dev.* **18**, 88-98.

Wolthuis, R., Clay-Farrace, L., van Zon, W., Yekezare, M., Koop, L., Ogink, J., Medema, R. and Pines, J. (2008). Cdc20 and Cks direct the spindle checkpoint-independent destruction of cyclin A. *Mol. Cell* **30**, 290-302.

Wu, T., Merbl, Y., Huo, Y., Gallop, J. L., Tzur, A. and Kirschner, M. W. (2010). UBE2S drives elongation of K11-linked ubiquitin chains by the anaphase-promoting complex. *Proc. Natl. Acad. Sci. USA* **107**, 1355-1360.

Yamamoto, A., Guacci, V. and Koshland, D. (1996). Pds1p, an inhibitor of anaphase in budding yeast, plays a critical role in the APC and checkpoint pathway(s). *J. Cell Biol.* **133**, 99-110.

Yoon, H. J., Feoktistova, A., Wolfe, B. A., Jennings, J. L., Link, A. J. and Gould, K. L. (2002). Proteomics analysis identifies new components of the fission and budding yeast anaphase-promoting complexes. *Curr. Biol.* **12**, 2048-2054.

Yoon, H. J., Feoktistova, A., Chen, J. S., Jennings, J. L., Link, A. J. and Gould, K. L. (2006). Role of Hcn1 and its phosphorylation in fission yeast anaphase-promoting complex/cyclosome function. *J. Biol. Chem.* **281**, 32284-32293.

Yu, H., King, R. W., Peters, J. M. and Kirschner, M. W. (1996). Identification of a novel ubiquitin-conjugating enzyme involved in mitotic cyclin degradation. *Curr. Biol.* **6**, 455-466.

Yu, H., Peters, J. M., King, R. W., Page, A. M., Hieter, P. and Kirschner, M. W. (1998). Identification of a cullin homology region in a subunit of the anaphase-promoting complex. *Science* **279**, 1219-1222.

Zachariae, W., Shin, T. H., Galova, M., Obermaier, B. and Nasmyth, K. (1996). Identification of subunits of the anaphase-promoting complex of Saccharomyces cerevisiae. *Science* **274**, 1201-1204.

Zachariae, W., Shevchenko, A., Andrews, P. D., Ciosk, R., Galova, M., Stark, M. J., Mann, M. and Nasmyth, K. (1998). Mass spectrometric analysis of the anaphase-promoting complex from yeast: identification of a subunit related to cullins. *Science* **279**, 1216-1219.

Zielke, N., Querings, S., Rottig, C., Lehner, C. and Sprenger, F. (2008). The anaphase-promoting complex/cyclosome (APC/C) is required for rereplication control in endoreplication cycles. *Genes Dev.* **22**, 1690-1703.

Zou, H., McGarry, T. J., Bernal, T. and Kirschner, M. W. (1999). Identification of a vertebrate sister-chromatid separation inhibitor involved in transformation and tumorigenesis. *Science* **285**, 418-422.

Zur, A. and Brandeis, M. (2001). Securin degradation is mediated by fzy and fzr, and is required for complete chromatid separation but not for cytokinesis. *EMBO J.* **20**, 792-801.

A

Calmodulin
Binding
Peptide

| Protein A | CBP | Human Mad2 |
| 15 kDa | 4 kDa | 24.3 kDa |

TEV Cleavage Site
Glu-Asn-Leu-Tyr-Phe-Gln-Glu

B

| EGFP | S Tag | Human BubR1 |
| 27 kDa | 15 AA | 120 kDa |

TEV Cleavage Site
Glu-Asn-Leu-Tyr-Phe-Gln-Glu

C

Roller bottle
HeLa cultures

Nocodazole   Lysate preparation
300 nM   ~ 10^{13} cells

IgG
Sepharose

TEV
protease

IgG
Sepharose

Ca^{2+}

Calmodulin
agarose

EDTA

MS/MS

D

Dish Hela Culture

Nocodazole   Lysate preparation
300 nM   ~ 10^{12} cells

Anti-GFP
Protein A
Sepharose

TEV
protease

Anti-GFP
Protein A
Sepharose

S-Protein
agarose

UREA

MS/MS

Alignment block 1

Species	Sequence
Homo Sapiens	MAASSSSSSAGGVSGSS-----VTGSGFS---VSDLAPPRKALFTY---PKGAGEMLE---D----------GSER---FLCES------
Mus musculus	MAASSSSSSAGGVSGSS-----VTGSGFS---VSDLAPPRKALFTY---PKGAGEMLE---D----------GSER---FLCES------
Monodelphis domestica	MAASSSSSSAGGVSGSS-----VTGSGFS---VSDLAPPRKALFTY---PKGAGEMLE---D----------GSER---FLCES------
Ornithorhynchus anatinus	MAASSSSSSAGGVSGSS-----VTGSGFS---VSDLAPPRKALFTY---PKGAGEMLE---G----------GSER---FLCES------
Gallus gallus	MAASSSSSSAGGVSGSS-----VTGSGFS---VSDLAPPRKALFTY---PKGAGEMLE---D----------GSER---FLCES------
Anolis carolinensis	MAASSSSSSAGGVSGSS-----VTGSGFS---VSDLATPRKALFTY---PKGAGEMLE---D----------GSER---FLCES------
Xenopus laevis	MAASSSSSSAGGVSGSS-----VTGSGLS---VSDLAPPRKALFTC---PKAAGEMLE---D----------GSER---FLCES------
Ambystoma mexicanum	MAASSSSSSAGGVSGSS-----ITGSGFS---VSDLVPPRKALFTT---PKGAGDLLE---D----------GSER---FLCES------
Danio rerio	MAASSSSSSAGGVSGSS-----VTGSGFS---ASELIPPRKVLYTY---PKGAGEMME---D----------GSDR---FLCES------
Lethenteron japonicum	MADLEAATRG-KTTT----------------SY---PA----PK---D----------VSDK---VLCDM------
Eptatretus burgeri	MAEGEAAGRVKA-------------------GVVGE------------NDRAK---VLCEL------
Branchiostoma floridae	MASVRNNPSNVEDVF----V--AMAAMAPRKALFQS---PKE-DEMVE---D----------GSQS---LVNKL------
Ciona intestinalis	MSRNAGTSSLSCKS---------LFSSGKSSKTN---PAAVEQTEE---D----SQHS---IHIA------
Saccoglossus kowalevskii	MATRGSPSSP------------ARNEPRKALFRS---PAPFEDN--Q--S----TPVIDH---VIAVL------
Paracentrotus lividus	MASFNRPSTSS----SS---ISGSGKP---WMATSPRKALFRS---PAATEDT-Q--S----AD---V---QFDKM------
Caligus rogercresseyi	MSSPSSPQASECSS-------F----LEDKHSPIRPVFSS---PGQIEDGGKGSGL---DNTNLEL---IMARH------
Drosophila melanogaster	MSSEASGSITIKEEAS-------TSGTATNIPVES---SEAEAKK---PEIGADKAES---QS------
Acanthoscurria gomesiana	MDNDSP--------------------LPRRALFQKRSLPRNIGDLTGS---DKDLPN---TKAKI------
Capitella capitata	MSSRTGGSPR-------------VELLDLRKALFSN---PAAAAAAAS---T----SKTTDA---LMNKL------
Lottia gigantea	MSNTTRTPKANG------------DHIRKALFMT---PVPENMRSSSS---S----NSNKLIN---IISKL------
Schmidtea mediterranea	MKSRNYYSYRP------------FNLRFKS---PLSLANFCSI---MTT-FSGFLTTSRME---LTLNP------
Caenorhabditis elegans	MALMYPFHVAQP------------PLNWS---EH---LWVSE---VSPAK
Ancylostoma caninum	MFSMMSNAESSPTTSSPFGFGSSSASPFSAPQTPDLD-DERSIYMS---PTPVSRSLKA-D----NVKE---IYFKA------
Nematostella vectnesis	MAAAKKKVAA-GD------------GLRKALFQS---PMTEEENAT---D----KTTEA---LLNKL------
Podocoryna carnea	MV------------KKELFKS---PASSANSN------EEIKA---FMKKT------
Trichoplax adhaerens	MSASVESSRKRRASS-------K----------------D---TCNSHSV---D----DQADS---IGIFM------
Arabidopsis thaliana	MKIHPLPRNENNNLI------HHA---RDPTREPGKKLRRL---PHIFSRVLEI---PLKSDADVAVEESHDCFRFVAETDGGGGG

Consensus: * — **AH1** PRKALFTY — **AH2** PKGAGEMLE — **AH3** GSER FLCES

Alignment block 2

Species	Sequence
Homo Sapiens	-VFSYQVASTLKQVKHDQQVARMEKLAGLVEELEADEWRFKPIEQLLG--------------------------FTPS--SG
Mus musculus	-VFSYQVASTLKQVKHDQQVARMEKLAGLVEELEADEWRFKPIEQLLG--------------------------FTPS--SG
Monodelphis domestica	-VFSYQVASTLKQVKHDQQVARMEKLAGLVEELEADEWRYKPIEQLLG--------------------------FTPS--SG
Ornithorhynchus anatinus	-VFSYQVASTLKQVKHGQQVARMEKLAGLVEELEADEWRYKPIEQLLG--------------------------FTPS--SG
Gallus gallus	-VFSYQVASTLKQVKHDQQVARMEKLAGLVEELEADEWRYKPIEQLLG--------------------------FTPS--SG
Anolis carolinensis	-VFSYQVASTLKQVKHDQQVARMEKLAGLVEELEADEWRYKPIEQLLG--------------------------FTPS--LG
Xenopus laevis	-VFSYQVASTLKQVKHDQQVSRMEKLAGLVEELEADEWRYTPIEQLLG--------------------------FTPS--SGGK
Ambystoma mexicanum	-VFSYQVASTLKQVKHDQQVSRMEKLAGLVEELEADEWRYTPIEQLLG--------------------------FTPS--SGGK
Danio rerio	-VFSYQVASTLKQVKHDQQVSRMERLAGLVEQLEADEWRYKPIEQLLG--------------------------FT----TS
Lethenteron japonicum	-IFNYQIAHTQREMNREQHCARLLKLARLAEELEADEWRFRPVEKLLG--------------------------FS-N--QS
Eptatretus burgeri	-FFKYEIAHNQREMKREQVCSQLRSLSRLADSLSEDEWRLPPAAQLTG----------------------------F--DS
Branchiostoma floridae	-MMDFDVASVRRSTNAELHQQRLNVLRLRLEETAADNWRYKPVDKLMG----------------------------L
Ciona intestinalis	-CKGTQVK---EELEKEKQEEQQIKDLKDLLITINQDNWKYKPIDELLG--------------------------L--S--SQ
Saccoglossus kowalevskii	-CVERDMEQCLKTTQKELHTHRLTQMRDLLGTLQENEWRYKPVEKLIG----------------------------L
Paracentrotus lividus	-EVEQLTENCVKNLQKEVNEQRLNDLRKKMVWLSETDWKYKRPEELIG--------------------------L----EK
Caligus rogercresseyi	-SFPDDVEKSLRAMQKEEHLKRMKNLRKSLEGLQKTEWQFTPINKLMG----------------------------Q
Drosophila melanogaster	----ETTEGGKAAETTENHLKRLQNLRKELSYLSETDWMYESLDKKAA----------------------------Q
Acanthoscurria gomesiana	-QFEHDLEASLRAFEKELHQQRLERLRQVAERLKEDSWRYPDIDNL----------------------------V
Capitella capitata	-QIEHDVEVSLAQFEKERHDQTVQELRLLEKVISDSNWRYTPIEKLIG----------------------------L
Lottia gigantea	-QLERDTEVFIKDGMKEAHEERLKELKDLVKTLEENDWRYPPVEKLLG--------------------------I----Q
Schmidtea mediterranea	-VMSISVFLIVSTFPSDS-EVPVLKLVILVKSLRLEHWDFVPLEQT--------------------------EPA--TD
Caenorhabditis elegans	ESFITTIC-EHRQAQWDNQ-DLLRHLQDSVAILTREDQRHVNAVHAAA--------------------------NMPA--NP
Ancylostoma caninum	-YVDEKLEVHKKELEEELHQGRMRALEQALEEAKKESWMYKPLD----------------------------F
Nematostella vectnesis	-QVEIEVDNNLTSLDKEMHEQRLSKLRKELDHNSQDEWKYKPIEQTIR----------------------------F
Podocoryna carnea	-DVEIEVDKNLKAVNKELHEKRINKMKQILEDSKKDDWKFEKIENLIG----------------------------Y
Trichoplax adhaerens	-RVDMEVDNFKEQYNKESLTEVMAGIKNVCQQLTKDEWKYRPINEI----------------------------I
Arabidopsis thaliana	GVRAYMVEIHPGVTKILVRTNGSSSLGLSLDELELDVWRFRLPESTRPELVTVDCDGDGELIVTVPKIEDNGRDLIVL--VQ

Consensus: : **AH4** MEKLAGLVEELEADEWRFKPIEQLLG

Acanthoscurria
Podocoryna
Ambystoma
Xenopus
Anolis
Gallus
Homo
Monodelphis
Mus
Ornithorhynchus
Danio
Branchiostoma
Nematostella
Trichoplax
Lethenteron
Capitella
Saccoglossus
Paracentrotus
Ancylostoma
Drosophila
Arabidopsis
Schmidtea
Caenorhabditis
Eptatretus
Caligus
Ciona
Lottia